ORGANOMETALLICS
Article
Cite This: Organometallics XXXX, XXX, XXX-XXX
pubs.acs.org/Organometallics

N-Benzoylbenzamidinate Complexes of Magnesium: Catalysts for the Ring-Opening Polymerization of ε-Caprolactone and CO_2/Epoxide Coupling

B. Raghavendra, K. Bakthavachalam, Buthanapalli Ramakrishna, and N. Dastagiri Reddy*

Department of Chemistry, Pondicherry University, Pondicherry 605 014, India

Supporting Information

ABSTRACT: A series of amidinate-based N,O-chelated magnesium complexes $[(L^1)_2(THF)_2Mg]$ (**1**), $[(L^2)_2(THF)_2Mg]$ (**2**), $[(L^3)_2(THF)_2Mg]$ (**3**), and $[(L^4)_2Mg]$ (**4**) were prepared by treating *N*-benzoyl-*N*′-arylbenzamidines ($L^{1-4}H$) with 0.5 equiv of di-*n*-butylmagnesium in THF. Analogous CH_3CN-coordinated complexes $[(L^1)_2(CH_3CN)_2Mg]$ (**5**) and $[(L^3)_2(CH_3CN)_2Mg]$ (**6**) were prepared in a similar way using CH_3CN as solvent. All of the compounds were characterized by $^1H/^{13}C$ NMR spectroscopy, and the molecular structures of **1**, **2**, and **4**–**6** were further confirmed by single-crystal X-ray diffraction studies. Complexes **1**, **2**, **5**, and **6** displayed good catalytic activity toward the ring-opening polymerization (ROP) of ε-caprolactone. In addition, **1**, **5**, and **6** were also found to be excellent catalysts for making cyclic carbonates from CO_2 and epoxides in the presence of a cocatalyst, *n*-Bu_4NBr.

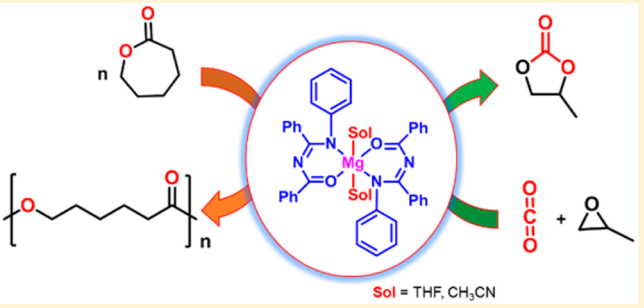

INTRODUCTION

Employing the coupling reaction of CO_2 and epoxide to generate cyclic/poly carbonates is not only 100% atom economical but also reduces the burden on nonrenewable resources used in the industry for making these highly important materials.[1] For example, CO_2, which is a renewable feedstock, contributes 43 kg to every 100 kg of the propylene carbonate produced by this method. Recently reported analyses on the production of poly/cyclic propylene carbonate from CO_2 and propylene oxide show that the process is sustainable, as it fixes the carbon on high-value chemicals, and may also be economically viable, depending upon the selling price of the product as well as the efficiency of the catalyst.[2] Owing to their high boiling points and polarity, cyclic carbonates have been used as polar aprotic solvents and as electrolytes in lithium ion batteries.[3] In addition to being intermediates[4] in the manufacture of fine chemicals, they also find applications in the cosmetics and plastics industries.[5] There are numerous main-group- and transition-metal-based catalysts reported for the synthesis of cyclic carbonates from CO_2 and epoxides.[6] Among these, Al and Mg have been attractive because not only are they nontoxic and earth-abundant but also they have afforded highly efficient catalysts with excellent turnover frequencies (TOFs).[6a,b] A few of these catalysts have also shown high activity in the production of polycaprolactone (PCL) via the ring-opening polymerization of ε-caprolactone.[7] PCL is a widely explored synthetic biodegradable and biocompatible polymer having a broad spectrum of biomedical and pharmaceutical applications.[8] Recently, we reported a few Al complexes of *N*-benzoyl-*N*′-arylbenzamidinates, which are highly active in the ROP of ε-caprolactone.[9] These complexes were found to be more active than the structurally analogous ketiminate Al complexes (Figure 1).[10] However, these Al complexes are not suitable for the synthesis of cyclic/poly carbonates, as they polymerize the epoxides to polyethers instantly. The enhanced activity of *N*-benzoyl-*N*′-arylbenzamidinate complexes can be attributed to the replacement of C by N in the ligand backbone, which makes the metal center more acidic. Encouraged by these results, we decided to synthesize magnesium complexes of these ligands and explore their catalytic efficiency toward CO_2/epoxide coupling and the ROP of ε-caprolactone. Herein, we describe in detail the synthesis and characterization of *N*-benzoyl-*N*′-arylbenzamidinate magnesium complexes and their catalytic activity.

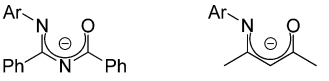

Figure 1. Isostructural features of *N*-benzoylbenzamidinate and ketiminate ligands.

RESULTS AND DISCUSSION

Synthesis and Structural Characterization of Proligands. *N*-Benzoyl-*N*′-phenylbenzamidine (L^1H) was synthe-

Received: August 11, 2017

DOI: 10.1021/acs.organomet.7b00617
Organometallics XXXX, XXX, XXX−XXX

sized by following a reported procedure, and the method was adopted for the preparation of analogous *N*-benzoyl-*N*′-arylbenzamidines (aryl = *p*-methoxyphenyl (L^2H), *p*-fluorophenyl (L^3H), *o*-methoxyphenyl (L^4H)) (Scheme 1).[11] The

Scheme 1. Synthesis of *N*-Benzoyl-*N*′-aryl-Substituted Benzamidines

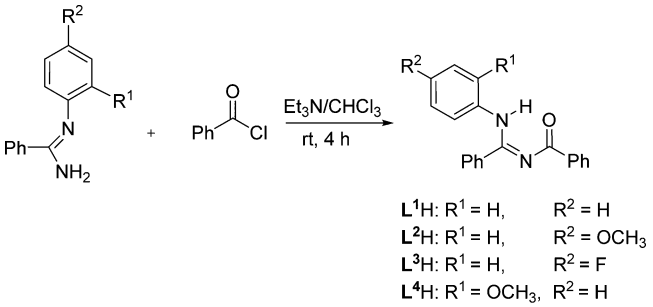

solid-state structures of L^2H, L^3H, and L^4H were determined by single crystal X-ray diffraction studies. The ORTEP diagrams and the bond parameters are given in the Supporting Information.

Synthesis and Structural Characterization of Magnesium Complexes. When the proligands L^1H, L^2H, L^3H, and L^4H were treated with di-*n*-butylmagnesium in a 2:1 molar ratio in THF, they afforded the magnesium complexes $[(L^1)_2(THF)_2Mg]$ (**1**), $[(L^2)_2(THF)_2Mg]$ (**2**), $[(L^3)_2(THF)_2Mg]$ (**3**), and $[(L^4)_2Mg]$ (**4**), respectively, in good yields (Scheme 2). $^1H/^{13}C$ NMR spectra of compounds **1**−**3** showed the presence of THF. The spectra correlate well with the solid-state molecular structures elucidated for complexes **1**, **2**, and **4** using single-crystal X-ray diffraction techniques. Single crystals of **3** suitable for X-ray analysis could not be obtained. The ORTEP diagrams depicting the molecular structures are shown in Figure 2, and their selected bond parameters are furnished in Table 1. In all of these complexes, Mg is in an octahedral geometry. In **1** and **2**, two molecules of THF coordinate to the metal in a *trans* fashion. The ligating atoms (N and O) in the chelating amidinate ligands also adopt a *trans* geometry. While there are no THF molecules in **4**, two positions are occupied by *o*-methoxy substituents in a *cis* fashion. The spatial arrangement of donor atoms around Mg reveals that the compound is a *fac* isomer. Surprisingly, neither the *mer* isomer nor the other possible *fac* isomer, where the methoxy groups are present in mutually *trans* positions, was obtained. This was confirmed by the NMR (^1H and ^{13}C) spectra of the bulk sample, which show only one resonance for the methoxy group. In **1** and **2**, all of the bond angles around the metal center are as per the ideal octahedral geometry, except for those present between the *cis* bonds in the equatorial plane. However, the bond angles at Mg in **4** suggest a considerable distortion in the octahedral geometry, as can be seen in the *trans* bonds, which deviate significantly from linearity (O2−Mg−O1 = 159° and N1−Mg−N1′ = 161°). The bite angles (O−Mg−N) of the six-membered chelates range from 82 to 85°, with the highest being found in **4**. The five-membered chelate rings present in **4** form the smallest bond angles around Mg (MeO−Mg−N = 74°). The Mg−N and Mg−O bond lengths are similar in all of the complexes and are in accordance with values for the reported magnesium complexes.[12]

Ring-Opening Polymerization of ε-Caprolactone.

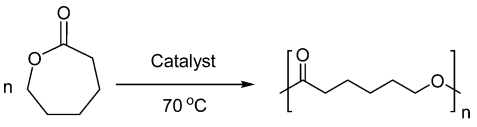

The catalytic abilities of complexes **1**−**4** in the ring-opening polymerization of ε-caprolactone were examined, and the results are summarized in Table 2. The ROP reactions were conducted neat at 70 °C without any cocatalyst. The resultant polymer was characterized by NMR, and the corresponding M_n and M_w values were obtained by gel permeation chromatography (GPC). In this paper, the terminology for catalytic activities has been used as per the classification given in Redshaw's review.[13] Complexes **1** and **2** show good activity and produced poly(caprolactone) in high yields within 30 min (Table 2, entries 1−10). Observed M_n values are in line with the calculated values. A linear relationship was established between the [CL]/[Mg] ratio and the number-averaged molecular weight (M_n) (Figures S2 and S3 in the Supporting Information). These observations suggest a well-controlled polymerization. Surprisingly, complexes **3** and **4** were found to be catalytically inactive under similar conditions. It is presumed that the THF molecules in **3** are strongly bound to the Mg center, which is more acidic than those in **1** and **2** due to the presence of the electron-withdrawing F atoms and hence ε-caprolactone cannot approach the metal center. Similarly, in **4**, dissociation of the MeO−Mg bond is difficult, as it is part of chelation. A similar observation has been reported in the

Scheme 2. Synthesis of Magnesium Complexes

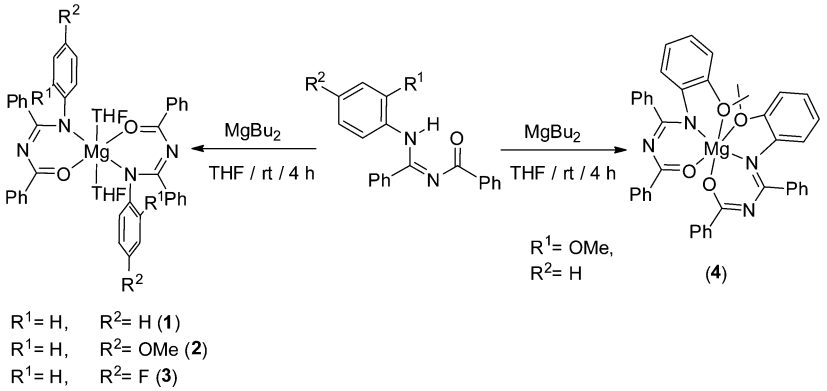

DOI: 10.1021/acs.organomet.7b00617
Organometallics XXXX, XXX, XXX−XXX

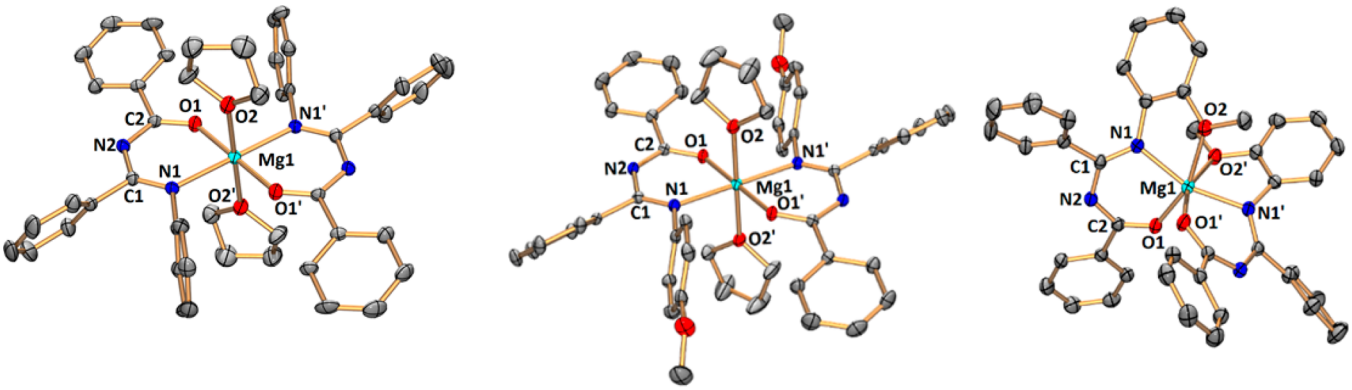

Figure 2. Single-crystal X-ray structures of **1**, **2**, and **4**. Hydrogen atoms are omitted for clarity. Thermal ellipsoids are drawn at the 40% probability level.

Table 1. Selected Bond Lengths and Bond Angles for 1, 2, and 4

	1	2	4
Bond Lengths (Å)			
Mg1−N1	2.170(4)	2.190(17)	2.103(19)
Mg1−O1	1.980(4)	1.979(14)	1.992(18)
Mg1−O2	2.132(4)	2.143(15)	2.183(18)
N1−C1	1.316(7)	1.304(3)	1.318(3)
C1−N2	1.353(7)	1.367(3)	1.350(3)
N2−C2	1.345(7)	1.322(3)	1.337(3)
C2−O1	1.242(6)	1.270(2)	1.265(3)
Bond Angles (deg)			
O1−Mg1−O1′	180.0	179.999(1)	96.83(11)
N1−Mg1−N1′	180.0	180.00(6)	161.00(12)
O2−Mg1−O1	89.08(18)	91.17(6)	159.08(6)
O2−Mg1−O2′	180.0	180.00(7)	86.21(10)
N1−Mg1−O1	82.76(16)	83.65(6)	85.02(7)

literature.[14] Kinetic experiments on the ROP of ε-caprolactone using **1** as the catalyst established an induction period of about 7 min (Figure 3). In order to reduce the induction period in **1** and to examine if the inactivity of **3** is due to the inert Mg−O(THF) bond, complexes with acetonitrile, which is a less basic ligand in comparison to THF, were synthesized and employed for the ROP. The complexes $[(L^1)_2(CH_3CN)_2Mg]$ (**5**) and $[(L^3)_2(CH_3CN)_2Mg]$ (**6**) have been characterized by NMR and single-crystal X-ray techniques. The molecular structures along with important bond parameters are given in Figure 4. The structural features and bond parameters are akin to those found in **1**−**3**. It is noteworthy that, in **5**, acetonitrile coordinates to Mg in a slightly bent fashion (Mg−N−C = 165°), whereas it is in linear coordination in **6** (Mg−N−C = 178°). The Mg−N(acetonitrile) bond distances also vary slightly. The bond is slightly shorter (2.236(13) Å) in **6** than in **5** (2.259(2) Å). These observations suggest that the acetonitrile is loosely bound in **5** in comparison to that in **6**, which was also

Table 2. ROP of ε-Caprolactone Initiated by 1−6[a]

entry	complex	[CL]/[Mg]	temp (°C)	time (min)	yield (%)[b]	M_n(GPC)[c]	M_n(calcd)[d]	TOF[e] (h^{-1})	PDI
1	**1**	100/1	70	30	98	13000	11000	196	1.53
2	**1**	200/1	70	30	96	17000	22000	384	1.77
3	**1**	300/1	70	30	94	29000	32000	564	1.62
4	**1**	400/1	70	30	90	39000	41000	720	1.82
5	**1**	500/1	70	30	87	46000	49000	870	1.88
6	**2**	100/1	70	30	97	12000	11000	194	1.53
7	**2**	200/1	70	30	95	18000	22000	380	1.58
8	**2**	300/1	70	30	92	32000	31000	552	1.90
9	**2**	400/1	70	30	88	38000	40000	704	1.84
10	**2**	500/1	70	30	86	46000	49000	860	1.65
11	**5**	100/1	70	5	99	11000	11000	1188	1.80
12	**5**	200/1	70	5	97	21000	22000	2328	1.59
13	**5**	300/1	70	5	95	39000	32000	3420	1.64
14	**5**	400/1	70	5	92	42000	42000	4416	1.90
15	**5**	500/1	70	5	90	64000	51000	5400	1.86
16	**6**	100/1	70	30	94	13000	11000	188	1.93
17	**6**	200/1	70	30	92	21000	21000	368	1.96
18	**6**	300/1	70	30	89	28000	30000	534	1.77
19	**6**	400/1	70	30	85	40000	39000	680	1.78
20	**6**	500/1	70	30	80	42000	45000	800	1.90

[a]0.02 mmol of catalyst. [b]Isolated yield. [c]Obtained from GPC analysis using a column calibrated by a polystyrene standard, multiplied by a correcting factor of 0.56.[15] [d]Theoretical M_n = (monomer/initiator) × (isolated yield) × (M_w of ε-CL). [e]Moles of ε-CL consumed per mole of catalyst per hour.

DOI: 10.1021/acs.organomet.7b00617
Organometallics XXXX, XXX, XXX−XXX

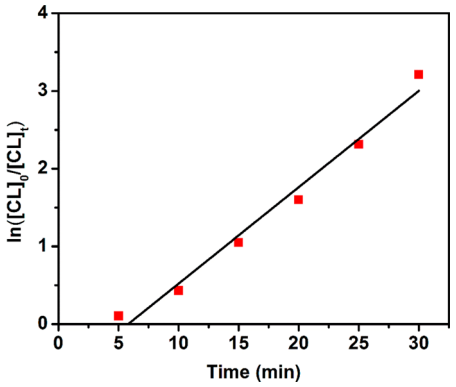

Figure 3. Plot of $\ln([CL]_0/[CL]_t)$ vs time for the polymerization of ε-CL catalyzed by **1**. Conditions: [CL]/[Mg] = 200/1 at 70 °C.

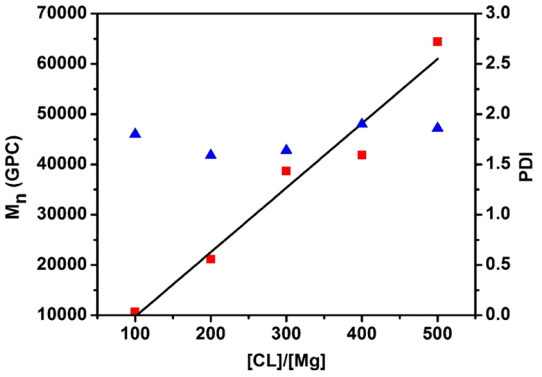

Figure 5. Plot of number-averaged molecular weight (M_n) and polydispersity index (PDI) vs [CL]/[Mg] for the polymerization of ε-CL using complex **5** at 70 °C (entries 11–15 in Table 2). Red squares (■) represent M_n (corrected) values, and blue triangles (▲) represent PDI values.

reflected in their catalytic activity. Eventually, **5** and **6** were used as catalysts in the ROP of ε-caprolactone. Complex **5** showed good activity and produced PCL in quantitative yield within 5 min (Table 2, entry 11). It also showed good tolerance to high monomer concentration and afforded 90% conversion (Table 2, entry 15, [CL]/[Mg] ratio = 500/1) within 5 min, leading to a very high TOF (>5400 h^{-1}). The fluoro-substituted complex **6** also showed good activity, though it took 30 min to polymerize 92% of CL when the [CL]/[Mg] ratio was 200/1. Agreement in the calculated and the observed M_n values suggest that both complexes catalyzed the ROP in a controlled manner. This was further confirmed by plotting [CL]/[Mg] ratios against the M_n values, which showed a linear relationship (Figure 5 for **5**, and Figure S4 in the Supporting Information for **6**).

These results clearly indicate that the solvent molecules, which coordinate to the metal center, can make a significant difference in the efficiency of the catalyst. Our attempts to synthesize Mg complexes of these N,O ligands ($\mathbf{L}^1$–$\mathbf{L}^3$) in toluene, in order to avoid solvent coordination, were unsuccessful. Catalytic efficiencies of these *N*-benzoyl-*N*′-arylbenzamidinate Mg complexes (**1**, **2**, **5**, and **6**) were compared with those of the structurally similar ketiminate Mg complexes reported in the literature, and it was found that the former were much more active than the latter. The ketiminate complexes took 3 h to polymerize 200 mol equiv of ε-CL. The higher efficiency in the *N*-benzoyl-*N*′-arylbenzamidinate complexes can be attributed to the increased acidity at the metal center as C is replaced by N in the ligand framework. A similar observation was made in our earlier work with Al complexes.[9] It has been observed that the efficiency of THF-coordinated Mg complex **1** is slightly less than that of [$\mathbf{L}^1$$AlMe_2$]. However, the acetonitrile-coordinated Mg complex **5** has been found to be much more active than the Al complex. **5** showed a TOF of 5400 h^{-1} when the [CL]/[M] ratio was 500, whereas the Al complex gave only 980 h^{-1} at this catalyst loading.[9]

Cycloaddition of CO_2 to Epoxides Catalyzed by Complexes 1, 5, and 6 in the Presence of *n*-Bu_4NBr. Complexes **1**, **3**, **5**, and **6** were examined as catalysts for the synthesis of propylene carbonate and cyclohexene carbonate

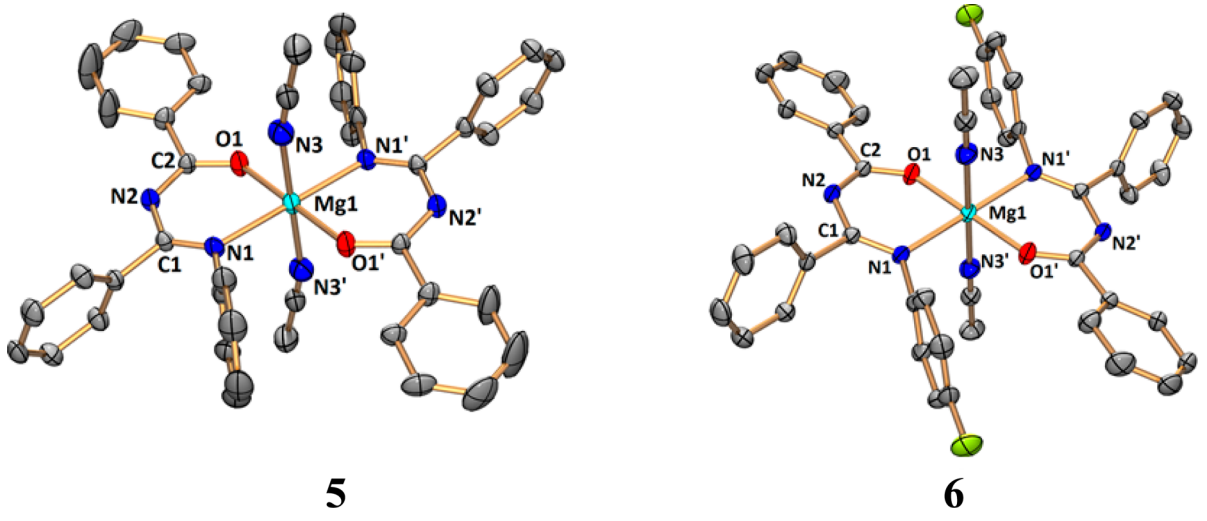

Figure 4. Single-crystal X-ray structures of **5** and **6**. Hydrogen atoms are omitted for clarity. Thermal ellipsoids are drawn at the 40% probability level. Selected bond lengths (Å) and bond angles (deg) for complex **5**: Mg1–N1 2.160(14), Mg1–O1 1.970(12), Mg1–N3 2.259(2); O1–Mg1–O1′ 180.0, N1–Mg1–N1′ 180.00(8), N3–Mg1–N3′ 180.0, N1–Mg1–O1 83.86(5). Selected bond lengths (Å) and bond angles (deg) for complex **6**: Mg1–N1 2.156(11), Mg1–O1 1.988(9), Mg1–N3 2.236(13); O1–Mg1–O1′ 180.00(4), N1–Mg1–N1′ 180.0, N3–Mg1–N3′ 180.0, N1–Mg1–O1 82.67(4).

DOI: 10.1021/acs.organomet.7b00617
Organometallics XXXX, XXX, XXX–XXX

from CO_2 and the corresponding epoxide (Scheme 3). The results of these experiments are given in Table 3. The reaction

Scheme 3. Synthesis of Cyclic Carbonates from Epoxides and CO_2 Using Complexes 1, 5, and 6

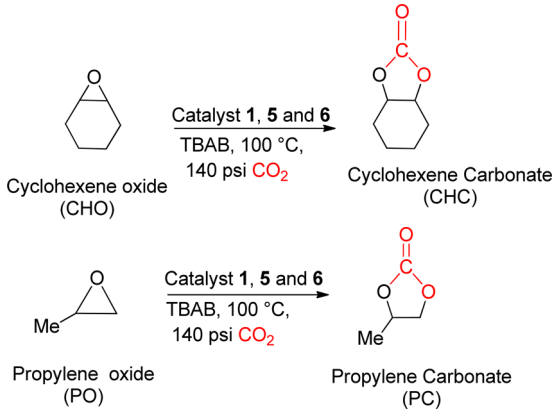

conditions were optimized by using **1** as a catalyst in the presence of a cocatalyst, n-Bu_4NX (X = Cl, Br, I) (Table 3, entries 1−3). It was observed that n-Bu_4NBr (TBAB) performed better than the iodide and the chloride at 100 °C at a CO_2 pressure of 140 psi. A similar observation was reported by Ko and co-workers.[7] Under these conditions, **1**/TBAB combination afforded 47% conversion of the epoxide into the cyclic carbonate in 13 h when a 1000/1 CHO/[Mg] ratio was used (entry 5, TON = 470). The conversion improved significantly (83%) when CH_3CN-coordinated complex **5** was employed (Table 3, entry 6). The TON reached 830. It may be recalled that, even in the ROP of ε-caprolactone, the performance of CH_3CN-coordinated complexes (**5** and **6**) was much higher than that of their THF-coordinated counterparts (**1** and **3**). **3**, having F substitution, was found to be inactive also in the coupling of CO_2 and CHO. However, the corresponding CH_3CN-coordinated complex **6** showed good activity. It afforded 55% conversion with a TON of 550 (Table 3, entry 7).

In order to cross-check the role of the catalyst and the cocatalyst, runs were carried out in their absence (Table 3, entries 8 and 9) and it was found that there was either no conversion or poor conversion of CHO. The complexes **1**, **5**, and **6** were also explored for their efficiency in catalyzing the CO_2/propylene oxide coupling reaction in the presence of n-Bu_4NBr at 100 °C at a CO_2 pressure of 140 psi. Catalyst **1** afforded 95% conversion of PO within 4 h even when the PO/[Mg] ratio was as high as 1000, leading to a TON of 950. However, when the ratio was increased to 2000/1 only a 51% conversion of PC with a TON of 1020 was observed (Table 3, entry 12). Complex **5** turned out to be superior to all the other complexes synthesized in this work and gave 96% conversion with a high TON (1920) when 2000 mol equiv of propylene oxide was used. With 4000 mol equiv of the monomer, the TON reached 2800 with a good conversion of PO (70%) (Table 3, entries 13 and 15).

CONCLUSION

Magnesium complexes supported by *N*-benzoyl-*N*′-arylbenzamidinate ligands were synthesized and structurally characterized. The complexes were examined for their catalytic activity in the synthesis of cyclic carbonates from CO_2 and epoxides (cyclohexene oxide and propylene oxide) and also in the ROP of ε-caprolactone. Complexes **1**, **2**, **5**, and **6** showed good activity toward the ROP of ε-caprolactone, while **3** and **4** were inactive. It is presumed that **3** is inactive because, in this complex, Mg is more acidic and less labile due to the presence of electron-withdrawing substituents (F atoms) on the ligand, which makes the dissociation of the Mg−O(THF) bond difficult. It was found that when THF was replaced by acetonitrile, which is less basic than THF, the complex (**6**) showed good activity. Complex **5**, which is the acetonitrile analogue of **1**, was found to be the best catalyst among all the complexes probed in this study. **1**, **5**, and **6** catalyzed the coupling reaction of CO_2 and cyclohexene/propylene oxide in the presence of TBAB and produced the corresponding cyclic carbonates in excellent yields with high TONs. **5** excelled in this reaction also and afforded propylene carbonate with a TON of 2800 within 4 h. Conversion of cyclohexene oxide took 13 h to achieve a TON of 830. A comparison of these results with the literature reports reveals that the catalysts **1**, **2**, **5**, and **6** show much higher activity in comparison to

Table 3. Coupling Reactions of Epoxide and CO_2 Catalyzed by Magnesium Complexes 1, 5, and 6

entry[a]	complex	epoxide	cocatalyst	epoxide/[Mg]	time (h)	conversn (%)[b]	TON[c]	TOF[d] (h^{-1})
1	**1**	CHO	TBAC	1000/1	6	22	220	36.6
2	**1**	CHO	TBAB	1000/1	6	25	250	41.6
3	**1**	CHO	TBAI	1000/1	6	20	200	33.3
4	**1**	CHO	TBAB	500/1	13	73	365	28.1
5	**1**	CHO	TBAB	1000/1	13	47	470	36.1
6	**5**	CHO	TBAB	1000/1	13	83	830	63.8
7	**6**	CHO	TBAB	1000/1	13	55	550	42.3
8[e]		CHO	TBAB	1000/0	13	3	30	2.3
9[f]	**1**	CHO		1000/1	13			
10[e]		PO	TBAB	1000/0	4	29	290	72
11	**1**	PO	TBAB	1000/1	4	95	950	237
12	**1**	PO	TBAB	2000/1	4	51	1020	255
13	**5**	PO	TBAB	2000/1	4	96	1920	480
14	**6**	PO	TBAB	2000/1	4	74	1480	370
15	**5**	PO	TBAB	4000/1	4	70	2800	700

[a]Reaction conditions: 0.02 mmol of initiator, CO_2 (140 psi), 100 °C. [b]Determined by ^1H NMR spectroscopy. [c]TON = (epoxide/[Mg] ratio) × (conversion)/100. [d]Overall turnover frequency (TON/reaction time in hours) observed. [e]Without catalyst. [f]Without cocatalyst.

DOI: 10.1021/acs.organomet.7b00617
Organometallics XXXX, XXX, XXX−XXX

structurally similar ketiminate magnesium complexes. This observation once again proves that *N*-benzoyl-*N*′-arylbenzamidinate ligands, which have N in the ligand framework, make the metal center more acidic, thereby increasing the catalytic efficiency of the complex.

EXPERIMENTAL SECTION

General Methods and Instrumentation. All manipulations were carried out using standard Schlenk line and glovebox techniques under an inert atmosphere of dry nitrogen. Di-*n*-butylmagnesium, benzoyl chloride, aniline, and aniline derivatives were procured from Aldrich and used as received. ε-Caprolactone, cyclohexene oxide, and propylene oxide were purchased from Acros Organics and dried over calcium hydride for 24 h before they were distilled under vacuum (CL) or nitrogen (PO and CHO). *N*-Phenylbenzamidine was prepared by following a literature procedure.[11,16] Tetrahydrofuran and toluene were freshly distilled from Na/benzophenone ketyl before use. Acetonitrile and $CDCl_3$ were distilled from calcium hydride. C_6D_6 was dried over sodium metal. ^1H and ^{13}C NMR spectra were recorded on a Bruker 400 MHz instrument. The molecular weights and the molecular weight distributions of the polymers were measured against polystyrene standards by GPC (gel permeation chromatography) using two Agilent PLGel columns 7.5 mm × 300 mm (5 μm pore size) at 20 °C and tetrahydrofuran as eluent. HRMS data were recorded on an Agilent 6540 UHD Q-TOF mass spectrometer. Elemental analyses were performed using a Thermo Scientific Flash 2000 CHNS analyzer.

X-ray Crystallographic Studies. Single crystals of **1**, **2**, and **4**−**6** were mounted on glass fibers in paraffin oil and then brought into the cold nitrogen stream of a low-temperature device so that the oil solidified. Data collection was performed on an OXFORD XCALIBUR diffractometer, equipped with a CCD area detector, using graphite-monochromated Mo Kα (λ = 0.71073 Å) radiation and a low-temperature device. Data collections for L^2H, L^3H, and L^4H were done at room temperature. All calculations were performed using SHELXS-97 and SHELXL-97.[17] The structures were solved by direct methods and successive interpretation of the difference Fourier maps, followed by full-matrix least-squares refinement (against F^2). All non-hydrogen atoms were refined anisotropically. The contributions of the hydrogen atoms, in their calculated positions, were included in the refinement using a riding model. Upon convergence, the final Fourier difference map of the X-ray structures showed no significant peaks. THF molecules that were present in the crystal lattice of **2** were highly disordered and could not be modeled from the difference Fourier electron density maps, and hence the SQUEEZE routine of PLATON was used to refine the structures. Relevant data concerning crystallographic data, data collection, and refinement details are summarized in Tables S1 and S2 in the Supporting Information. Crystallographic information files (CIF) for the structures reported in this paper have been deposited with the Cambridge Crystallographic Data Centre as supplementary publication nos. 1510720 (L^2H), 1537239 (L^3H), 1510719 (L^4H), 1429057(**1**), 1429062 (**2**), 1429056 (**4**), 1511002 (**5**), and 1537020 (**6**). Copies of the data can be obtained free of charge on application to the CCDC, 12 Union Road, Cambridge CB2 1EZ, U.K. (fax, (+44) 1223-336-033; e-mail, deposit@ccdc.cam.ac.uk).

General Procedure for the Preparation of Proligands (L^2H, L^3H, and L^4H). The synthetic procedure was adopted from the literature.[11] To a solution of *N*-arylbenzamidine in chloroform was added triethylamine at room temperature. The reaction mixture was cooled to 0 °C followed by the addition of benzoyl chloride. The resultant turbid solution was stirred for 4 h at room temperature before it was washed with an excess of dilute sodium carbonate solution. The chloroform portion was separated, dried over anhydrous Na_2SO_4, and evaporated in vacuo. The resultant gummy residue was purified by recrystallization (see below).

L^2H. **1b** (2.00 g, 8.84 mmol), triethylamine (1.07 g, 10.61 mmol), benzoyl chloride (1.36 g, 9.73 mmol), and chloroform (30 mL) were used. Colorless crystals of L^2H were obtained from a solution of the residue in a hexane/dichloromethane mixture at room temperature. Yield: 79% (2.30 g). Mp: 108−110 °C. ^1H NMR ($CDCl_3$, 400 MHz): δ 12.54 (br, 1H, NH), 8.35 (d, 2H, Ar H), 7.62−7.60 (d, 2 H, Ar H), 7.54−7.51 (t, 1H, Ar H), 7.47−7.39 (m, 3H, Ar H) 7.34−7.30 (t, 2H, Ar H), 6.96 (d, 2H, Ar H), 6.76 (d, 2H, Ar H), 3.74 (s, 3H, OCH_3). ^{13}C NMR ($CDCl_3$, 100 MHz): δ 179.63, 157.59, 137.36, 134.64, 132.17, 130.94, 129.69, 128.34, 128.20, 125.37, 114.36, 55.46. HRMS (ESI): *m*/*z* calcd for $C_{21}H_{19}N_2O_2$ $[M + H]^+$ 331.1446, found 331.1440. Anal. Calcd for $C_{21}H_{18}N_2O_2$: C, 76.34; H, 5.49; N, 8.48. Found: C, 76.52; H, 5.54; N, 8.67.

L^3H. **1c** (1.60 g, 7.47 mmol), triethylamine (0.90 g, 8.97 mmol), benzoyl chloride (1.15 g, 8.22 mmol), and chloroform (25 mL) were used. Pale yellow crystals of L^3H were obtained from a solution of the residue in a hexane/dichloromethane mixture at room temperature. Yield: 81% (1.91 g). Mp: 112−114 °C. ^1H NMR ($CDCl_3$, 400 MHz): δ 11.99 (br, 1H, NH), 8.30 (d, 2H, Ar H), 7.58−7.55 (m, 2H, Ar H), 7.53−7.51 (m, 1H, Ar H), 7.47−7.40 (m, 3H, Ar H), 7.40−7.31 (m, 2H,Ar H), 7.04−7.02(m, 2H, Ar H), 7.01−6.91 (m, 2H, Ar H). ^{13}C NMR ($CDCl_3$, 100 MHz): δ 179.38, 161.65, 159.21, 136.98, 134.31, 132.43, 131.21, 129.75, 129.57, 128.54, 128.32, 125.48, 125.40, 116.19, 115.96. HRMS (ESI): *m*/*z* calcd for $C_{20}H_{16}N_2OF$ $[M + H]^+$ 319.1246, found 319.1240. Anal. Calcd for $C_{20}H_{15}N_2OF$: C, 75.46; H, 4.75; N, 8.80. Found: C, 75.85; H, 4.77; N, 8.48.

L^4H. **1d** (1.20 g, 5.30 mmol), triethylamine (0.64 g, 6.37 mmol), benzoyl chloride (0.82 g, 5.84 mmol), and chloroform (30 mL) were used. Pale yellow crystals of L^4H were obtained from a solution of the residue in a toluene/hexane mixture at 0 °C. Yield: 86% (1.50 g). Mp: 127−129 °C. ^1H NMR ($CDCl_3$, 400 MHz): δ 10.64 (br, 1H, NH), 8.29 (d, 2H, Ar H), 7.58−7.57 (d, 2H, Ar H), 7.54−7.50 (t, 1H, Ar H), 7.46−7.41 (m, 4H, Ar H), 7.37−7.33 (t, 2H, Ar H), 7.12−7.08 (t, 1H, Ar H), 6.91−6.83 (d, 2H, Ar H), 3.87 (s, 3H, OCH_3). ^{13}C NMR ($CDCl_3$, 100 MHz): δ 178.56, 150.36, 136.93, 135.13, 132.25, 131.05, 129.81, 128.64, 128.30, 128.02, 125.72, 123.17, 120.74, 110.78, 55.84. HRMS (ESI): *m*/*z* calcd for $C_{21}H_{19}N_2O_2$ $[M + H]^+$ 331.1446, found 331.1438. Anal. Calcd for $C_{21}H_{18}N_2O_2$: C, 76.34; H, 5.49; N, 8.48. Found: C, 76.77; H, 5.52; N, 8.81.

General Procedure for the Preparation of Magnesium Complexes. To a solution of L^1H−L^4H in tetrahydrofuran or acetonitrile was added $MgBu_2$ at 0 °C. The reaction mixture was warmed to reach room temperature and stirred for 4 h. The resultant solid was collected by filtration and dried under vacuum to obtain a white or pale yellow solid.

*$[(L^1)_2(THF)_2Mg]$ (**1**)*. L^1H (0.32 g, 1.06 mmol), tetrahydrofuran (10 mL), and $MgBu_2$ (0.53 mL, 1 M in heptane, 0.53 mmol) were used. Colorless crystals were grown from hot tetrahydrofuran. Yield: 83% (0.34 g). Mp: 147−149 °C. ^1H NMR ($CDCl_3$, 400 MHz): δ 7.84 (d, 4H, Ar H), 7.38−7.34 (t, 10H, Ar H), 7.24−7.13 (d, 6H, Ar H), 7.03 (s, 4H, Ar H), 6.86 (s, 6H, Ar H), 3.85 (t, 8H, OCH_2CH_2), 1.85 (m, 8H, OCH_2CH_2). ^{13}C NMR ($CDCl_3$, 100 MHz): δ 172.85, 171.38, 151.01, 140.73, 139.20, 130.60, 129.77, 129.67, 128.17, 127.90, 127.68, 127.45, 127.23, 125.16, 123.00, 68.67, 25.61.

*$[(L^2)_2(THF)_2Mg]$ (**2**)*. L^2H (0.41 g, 1.24 mmol), tetrahydrofuran (10 mL), and $MgBu_2$ (0.62 mL, 1 M in heptane, 0.62 mmol) were used. Colorless crystals were grown from hot tetrahydrofuran. Yield: 77% (0.39 g). Mp: 233−235 °C. ^1H NMR ($CDCl_3$, 400 MHz): δ 7.85 (s, 4H, Ar H), 7.32 (s, 6H, Ar H), 7.24 (s, 4H, Ar H), 7.12 (s, 6H, Ar H), 6.70 (s, 4H, Ar H), 6.51 (s, 4H, Ar H), 3.83 (t, 11H, OCH_2CH_2), 3.54 (s, 6H, OCH_3) 1.86 (q, 11H, OCH_2CH_2). ^{13}C NMR ($CDCl_3$, 100 MHz): δ 172.63, 171.01, 155.45, 144.12, 140.93, 139.63, 130.35, 129.75, 129.56, 128.64, 127.62, 127.33, 127.26, 126.84, 125.72, 113.42, 68.47, 55.21, 25.66.

*$[(L^3)_2(THF)_2Mg]$ (**3**)*. L^3H (0.30 g, 0.94 mmol), tetrahydrofuran (10 mL), and $MgBu_2$ (0.47 mL, 1 M in heptane, 0.47 mmol) were used. Yield: 74% (0.27 g). Mp: 160−163 °C. ^1H NMR ($CDCl_3$, 400 MHz): δ 7.86 (d, 4H, Ar H), 7.40−7.27 (m, 10H, Ar H), 7.14 (d, 6H, Ar H), 6.72 (d, 8H, Ar H), 3.86 (s, 8H, OCH_2CH_2), 1.87 (t, 8H, OCH_2CH_2). ^{13}C NMR ($CDCl_3$, 100 MHz): δ 173.05, 171.74, 160.42, 158.01, 147.02, 145.37, 140.54, 139.08, 130.82, 129.66, 129.50, 128.79, 128.96, 128.77, 128.29, 128.09, 128.00, 127.57, 127.41, 126.19, 126.12, 125.36, 116.45, 116.23, 114.91, 114.69, 68.68, 25.67.

DOI: 10.1021/acs.organomet.7b00617
Organometallics XXXX, XXX, XXX−XXX

[(L^4)$_2$Mg] (4). L^4H (0.45 g, 1.36 mmol), tetrahydrofuran (10 mL), and $MgBu_2$ (0.68 mL, 1 M in heptane, 0.68 mmol) were used. Colorless crystals were grown from tetrahydrofuran. Yield: 85% (0.39 g). Mp: 181−183 °C. ^{1}H NMR ($CDCl_3$, 400 MHz): δ 8.11−8.09 (m, 4H, Ar H), 7.77−7.75 (m, 4H, Ar H), 7.39−7.33 (m, 8H, Ar H), 7.27−7.23 (m, 4H, Ar H), 6.90−6.82 (m, 4H, Ar H), 6.70−6.68(m, 2H, Ar H), 6.67−6.54 (m, 2H, Ar H), 3.86 (s, 6H, OCH_3). ^{13}C NMR ($CDCl_3$, 100 MHz): δ 174.66, 171.48, 149.83, 139.20, 138.52, 137.91, 131.22, 130.36, 129.81, 129.76, 128.31, 127.76, 124.57, 123.18, 122.21, 110.33, 55.98.

[(L^1)$_2$(CH_3CN)$_2$Mg] (5). L^1H (0.50 g, 1.66 mmol), acetonitrile (10 mL), and $MgBu_2$ (0.83 mL, 1 M in heptane, 0.83 mmol) were used. Colorless crystals were grown from acetonitrile. Yield: 88% (0.51 g). Mp: 242−244 °C. ^{1}H NMR ($CDCl_3$, 400 MHz): δ 7.69 (s, 4H, Ar H), 7.30 (s, 2H, Ar H), 7.10−7.03 (m, 14H, Ar H), 6.81−6.72 (d, 7H, Ar H), 6.46 (s, 3H, Ar H), 1.98 (s, 6H, CH_3CN). ^{13}C NMR ($CDCl_3$, 100 MHz): δ 171.79, 148.69, 138.51, 137.59, 130.90, 129.74, 129.54, 128.22, 127.46, 127.24, 124.79, 123.85, 116.55, 2.02.

[(L^3)$_2$(CH_3CN)$_2$Mg] (6). L^3H (0.41 g, 1.28 mmol), acetonitrile (10 mL), and $MgBu_2$ (0.64 mL, 1 M in heptane, 0.64 mmol) were used. Colorless crystals were grown from hot acetonitrile. Yield: 87% (0.415 g). Mp: 171−173 °C. ^{1}H NMR ($CDCl_3$, 400 MHz): δ 7.92 (s, 4H, Ar H), 7.37 (s, 2H, Ar H), 7.21 (s, 4H, Ar H), 7.06−6.99 (t, 10H, Ar H) 6.50−6.32 (t, 8H, Ar H), 1.92 (s, 6H, CH_3CN). ^{13}C NMR ($CDCl_3$, 100 MHz): δ 172.64, 172.24, 160.64, 158.22, 144.92, 138.36, 137.66, 131.19, 129.75, 129.29, 128.53, 128.38, 127.63, 127.42, 127.19, 126.06, 126.01, 116.61, 114.88, 114.66, 1.87.

General Procedure for the Ring-Opening Polymerization of ε-CL. A Schlenk flask was charged with the catalyst and ε-caprolactone in a glovebox, and the solution was stirred for 5−30 min at 70 °C. The polymerization reaction was terminated by addition of several drops of glacial acetic acid (∼0.2 mL) into the reaction mixture. The resultant viscous solution was diluted with dichloromethane and transferred into a flask containing cold methanol (60 mL) with stirring. The precipitated polymer was collected by filtration, washed with cold methanol, and dried under vacuum.

General Procedure for the Insertion of CO_2 into Epoxides. In a typical procedure for the cycloaddition of CO_2 to epoxide, the catalyst, the epoxide, and the quaternary ammonium salt were taken in a 50 mL high-pressure reactor in a glovebox. The reactor was brought out, pressurized with CO_2, and kept in an oil bath maintained at 100 °C, and the contents were stirred using a magnetic stirrer. After the completion of the reaction time, the reactor was cooled in an ice bath before the excess pressure was slowly released. The resultant mixture was analyzed using ^{1}H NMR.

■ ASSOCIATED CONTENT

Ⓢ Supporting Information

The Supporting Information is available free of charge on the ACS Publications website at DOI: 10.1021/acs.organomet.7b00617.

Crystallographic data for L^2H, L^3H, L^4H, **1**, **2**, and **4**−**6**, single-crystal X-ray structures of L^2H, L^3H, and L^4H, and ^{1}H and ^{13}C NMR spectra of all compounds (PDF)

Accession Codes

CCDC 1429056−1429057, 1429062, 1510719−1510720, 1511002, 1537020, and 1537239 contain the supplementary crystallographic data for this paper. These data can be obtained free of charge via www.ccdc.cam.ac.uk/data_request/cif, or by emailing data_request@ccdc.cam.ac.uk, or by contacting The Cambridge Crystallographic Data Centre, 12 Union Road, Cambridge CB2 1EZ, UK; fax: +44 1223 336033.

■ AUTHOR INFORMATION

Corresponding Author

*E-mail for N.D.R.: ndreddy.che@pondiuni.edu.in.

ORCID

Buthanapalli Ramakrishna: 0000-0002-8967-6167

N. Dastagiri Reddy: 0000-0003-2290-9445

Notes

The authors declare no competing financial interest.

■ ACKNOWLEDGMENTS

We gratefully acknowledge the Department of Science and Technology (DST), New Delhi, India, for financial support and the Alexander von Humboldt Stiftung, Germany, for the donation of a glovebox. B.R. thanks the University Grants Commission for a fellowship. We thank the Central Instrumentation Facility, Pondicherry University, for NMR spectra and DST-FIST for the single-crystal X-ray diffraction facility.

■ REFERENCES

(1) Shaikh, A.-A. G.; Sivaram, S. *Chem. Rev.* **1996**, *96*, 951−976.

(2) Demirel, Y. *J. Chem. Eng. Process Technol.* **2015**, *6*, DOI: 10.4172/2157-7048.1000236.

(3) (a) Schäffner, B.; Schäffner, F.; Verevkin, S. P.; Börner, A. *Chem. Rev.* **2010**, *110*, 4554−4581. (b) Sakakura, T.; Kohno, K. *Chem. Commun.* **2009**, 1312−1330.

(4) Clements, J. H. *Ind. Eng. Chem. Res.* **2003**, *42*, 663−674.

(5) (a) Nohra, B.; Candy, L.; Blanco, J.-F.; Guerin, C.; Raoul, Y.; Mouloungui, Z. *Macromolecules* **2013**, *46*, 3771−3792. (b) Carré, C.; Bonnet, L.; Avérous, L. *RSC Adv.* **2015**, *5*, 100390−100400. (c) Besse, V.; Camara, F.; Voirin, C.; Auvergne, R.; Caillol, S.; Boutevin, B. *Polym. Chem.* **2013**, *4*, 4545−4561.

(6) (a) Maeda, C.; Shimonishi, J.; Miyazaki, R.; Hasegawa, J.-Y.; Ema, T. *Chem. - Eur. J.* **2016**, *22*, 6556−6563. (b) Cuesta-Aluja, L.; Castilla, J.; Masdeu-Bultó, A. M. *Dalton Trans.* **2016**, *45*, 14658−14667. (c) Kim, S. H.; Ahn, D.; Go, M. J.; Park, M. H.; Kim, M.; Lee, J.; Kim, Y. *Organometallics* **2014**, *33*, 2770−2775. (d) Luo, R.; Zhou, X.; Zhang, W.; Liang, Z.; Jiang, J.; Ji, H. *Green Chem.* **2014**, *16*, 4179−4189. (e) Rulev, Y. A.; Larionov, V. A.; Lokutova, A. V.; Moskalenko, M. A.; Lependina, O. L.; Maleev, V. I.; North, M.; Belokon, Y. N. *ChemSusChem* **2016**, *9*, 216−222. (f) Alhashmialameer, D.; Collins, J.; Hattenhauer, K.; Kerton, F. M. *Catal. Sci. Technol.* **2016**, *6*, 5364−5373. (g) Al-Qaisi, F.; Streng, E.; Tsarev, A.; Nieger, M.; Repo, T. *Eur. J. Inorg. Chem.* **2015**, *2015*, 5363−5367. (h) Babu, H. V.; Muralidharan, K. *RSC Adv.* **2014**, *4*, 6094−6102. (i) Lu, X.-B.; Liang, B.; Zhang, Y.-J.; Tian, Y.-Z.; Wang, Y.-M.; Bai, C.-X.; Wang, H.; Zhang, R. *J. Am. Chem. Soc.* **2004**, *126*, 3732−3733. (j) Ren, W.-M.; Liu, Y.; Lu, X.-B. *J. Org. Chem.* **2014**, *79*, 9771−9777.

(7) Li, C.-Y.; Wu, C.-R.; Liu, Y.-C.; Ko, B.-T. *Chem. Commun.* **2012**, *48*, 9628−9630.

(8) (a) Agarwal, S.; Wendorff, J. H.; Greiner, A. *Polymer* **2008**, *49*, 5603−5621. (b) Ikada, Y.; Tsuji, H. *Macromol. Rapid Commun.* **2000**, *21*, 117−132. (c) Khan, N. *Studies by Undergraduate Researchers at Guelph*; University of Guelph: Guelph, 2012; Vol. *5*, pp 63−73. (d) Chen, H.; Bai, S.; Chen, Y. *Tissue Eng. Regener. Med.* **2012**, *9*, 109−115. (e) Shevach, M.; Maoz, B. M.; Feiner, R.; Shapira, A.; Dvir, T. *J. Mater. Chem. B* **2013**, *1*, 5210−5217.

(9) (a) Bakthavachalam, K.; Rajagopal, A.; Reddy, N. D. *Dalton Trans.* **2014**, *43*, 14816. (b) Bakthavachalam, K.; Reddy, N. D. *Organometallics* **2013**, *32*, 3174−3184.

(10) (a) Yu, R.-C.; Hung, C.-H.; Huang, J.-H.; Lee, H.-Y.; Chen, J.-T. *Inorg. Chem.* **2002**, *41*, 6450−6455. (b) Altaf, C. T.; Wang, H.; Keram, M.; Yang, Y.; Ma, H. *Polyhedron* **2014**, *81*, 11−20.

(11) (a) Peak, D. A. *J. Chem. Soc.* **1952**, 215−226. (b) Cooper, F. C.; Partridge, W.; Short, W. F. *J. Chem. Soc.* **1951**, 391−404. (c) Wigbers, C.; Prigge, J.; Mu, Z.; Fröhlich, R.; Chi, L.; Würthwein, E.-U. *Eur. J. Org. Chem.* **2011**, *2011*, 861−877.

(12) Lee, W.-Y.; Hsieh, H.-H.; Hsieh, C.-C.; Lee, H. M.; Lee, G.-H.; Huang, J.-H.; Wu, T.-C.; Chuang, S.-H. *J. Organomet. Chem.* **2007**, *692*, 1131−1137.

DOI: 10.1021/acs.organomet.7b00617
Organometallics XXXX, XXX, XXX−XXX

(13) Arbaoui, A.; Redshaw, C. *Polym. Chem.* **2010**, *1*, 801−826.
(14) Hung, W.-C.; Lin, C.-C. *Inorg. Chem.* **2009**, *48*, 728−734.
(15) Save, M.; Schappacher, M.; Soum, A. *Macromol. Chem. Phys.* **2002**, *203*, 889−899.
(16) (a) Maheswari, K.; Rajendran, N. M.; Meyer, J.; Reddy, N. D. *Organometallics* **2010**, *29*, 3799−3807. (b) Maheswari, K.; Reddy, N. D. *Organometallics* **2012**, *31*, 197−206.
(17) Sheldrick, G. M. *Acta Crystallogr., Sect. A: Found. Crystallogr.* **2008**, *64*, 112−122.

DOI: 10.1021/acs.organomet.7b00617
Organometallics XXXX, XXX, XXX−XXX